Assessment of *p-y* Curves from Numerical Methods for a Non-Slender Monopile in Cohesionless Soil

Torben Kirk Wolf
Kristian Lange Rasmussen
Mette Hansen
Hanne Ravn Roesen
Lars Bo Ibsen

ISSN 1901-7278
DCE Technical Memorandum No. 024

AALBORG UNIVERSITY
Department of Civil Engineering

Aalborg University
Department of Civil Engineering

DCE Technical Memorandum No. 024

Assessment of *p-y* Curves from Numerical Methods for a Non-Slender Monopile in Cohesionless Soil

by

Torben Kirk Wolf
Kristian Lange Rasmussen
Mette Hansen
Hanne Ravn Roesen
Lars Bo Ibsen

June 2013

Scientific Publications at the Department of Civil Engineering

Technical Reports are published for timely dissemination of research results and scientific work carried out at the Department of Civil Engineering (DCE) at Aalborg University. This medium allows publication of more detailed explanations and results than typically allowed in scientific journals.

Technical Memoranda are produced to enable the preliminary dissemination of scientific work by the personnel of the DCE where such release is deemed to be appropriate. Documents of this kind may be incomplete or temporary versions of papers—or part of continuing work. This should be kept in mind when references are given to publications of this kind.

Contract Reports are produced to report scientific work carried out under contract. Publications of this kind contain confidential matter and are reserved for the sponsors and the DCE. Therefore, Contract Reports are generally not available for public circulation.

Lecture Notes contain material produced by the lecturers at the DCE for educational purposes. This may be scientific notes, lecture books, example problems or manuals for laboratory work, or computer programs developed at the DCE.

Theses are monograms or collections of papers published to report the scientific work carried out at the DCE to obtain a degree as either PhD or Doctor of Technology. The thesis is publicly available after the defence of the degree.

Latest News is published to enable rapid communication of information about scientific work carried out at the DCE. This includes the status of research projects, developments in the laboratories, information about collaborative work and recent research results.

Published 2013 by
Aalborg University
Department of Civil Engineering
Sohngaardsholmsvej 57,
DK-9000 Aalborg, Denmark

Printed in Aalborg at Aalborg University

ISSN 1901-7278
DCE Technical Memorandum No. 024

Assessment of *p-y* Curves from Numerical Methods for a Non-Slender Monopile in Cohesionless Soil

T. K. Wolf [2], K. L. Rasmussen[3], M. Hansen[2], L. B. Ibsen[1] and H. R. Roesen[1],
[1]Department of Civil Engineering, Aalborg University, Denmark
[2] COWI, Lyngby, Denmark
[3] Niras, Aalborg, Denmark

ABSTRACT

In current design the monopile is a widely used solution as foundation of offshore wind turbines. Winds and waves subject the monopile to considerable lateral loads. The behaviour of monopiles under lateral loading is not fully understood and the current design guidances apply the *p-y* curve method in a Winkler model approach. The *p-y* curve method was originally developed for jag-piles used in the oil and gas industry which are much more slender than the monopile foundation. In recent years the 3D finite element analysis has become a tool in the investigation of complex geotechnical situations, such as the laterally loaded monopile. In this paper a 3D FEA is conducted as basis of an extraction of *p-y* curves, as a basis for an evaluation of the traditional curves. Two different methods are applied to create a list of data points used for the *p-y* curves: A force producing a similar response as seen in the ULS situation is applied stepwise; hereby creating the most realistic soil response. This method, however, does not generate sufficient data points around the rotation point of the pile. Therefore, also a forced horizontal displacement of the entire pile is applied, whereby displacements are created over the entire length of the pile. The response is extracted from the interface and the nearby soil elements respectively, as to investigate the influence this has on the computed curves. *p-y* curves are obtained near the rotation point by evaluation of soil response during a prescribed displacement but the response is not in clear agreement with the response during an applied load.Two different material models are applied. It is found that the applied material models have a significant influence on the stiffness of the evaluated *p-y* curves. The *p-y* curves evaluated by means of FEA are compared to the conventional *p-y* curve formulation which provides a much stiffer response. It is found that the best response is computed by implementing the Hardening Soil model and extracting the data from the interface. There is a significant difference in the response from the two applied mechanisms. However, only the forced horizontal displacement provides meaningful data near the rotation point of the pile.

INTRODUCTION

The design of laterally loaded monopiles in current design regulations i.e. Det Norske Veritas (DNV, 2010) and American Petroleum Institute (API, 2010) is done by means of the *p-y* curve method. The pile-soil behaviour is modelled by a Winkler model approach where the pile is modelled as a beam supported by uncoupled springs. The springs represent the response of the soil and the spring stiffnesses are modelled by *p-y* curves which account for the non-linear relationship between soil resistance and lateral deflection of the pile. The *p-y* curve theory was initially developed for piles in the oil and gas industry and is based on test results from slender, flexible piles. Thus, the curves were not developed for piles with diameters of 4 to 6 m which are often used for the foundation of wind turbines today. No approved method exists for the design of large diameter piles and therefore the *p-y* curve method is still the applied method today.

Previous Studies

In the *p-y* curve method a number of parameters are not clarified when considering large diameter piles. Some of these limitations have been elaborated in a literature study by Sørensen el al. (2012). Several studies have been made to investigate the behaviour of large diameter piles under lateral loading. Sørensen el al. (2009) conducted a finite element (FE) analysis supported by a series of scaled tests and found that the initial stiffness of the *p-y* curve increases with pile diameter. This is supported by Moreno et al. (2011) who made similar studies. Hald et al. (2009) studied a full-scale monopile, 4 m in diameter, at Horns Rev and concluded that the *p-y* curves underestimate the soil strength at the top of the pile. It was found that the measured response at the top of the pile was 30-50 % smaller than that predicted by the *p-y* curves. McGann et al. (2011) found that the initial stiffness of the *p-y* curves and the ultimate lateral resistance at depths is overestimated compared to FE models.

In order to consider the actual three dimensional interaction between pile and soil a 3D FE-analysis can be performed. The FE-analysis considers factors such as shear forces, soil-pile interaction, layered soil, coefficient of lateral earth pressure, and soil dilatancy. Most FE studies have been made by means of the Mohr-Coulomb material model (MC), but Moreno et al. (2011) found that the Hardening Soil model (HS) is more suited when comparing the results with small scale tests in a pressure tank. The Hardening Soil model employs an elasto-plastic behaviour and considers the stress dependent stiffness of the soil and the effects of isotropic hardening. Moreno et al. (2011) found that the more extensive Hardening Soil Small Strains model is only slightly

more accurate than the Hardening Soil model when considering laterally loaded piles. Considering the extra computational effort they did not recommend the Hardening Soil Small Strains model. By extracting the pile-soil response in the generated model improved *p-y* curves can be formulated. A method proposed by Fan and Long (2005) is used for extracting soil resistance from stresses in the pile-soil interface elements. Their paper is however not descriptive regarding the evaluation of the stresses.

Subjects of Interest

In the literature numerous finite element analyses have been performed in order to create more reliable *p-y* curves. However, there is a lack of knowledge regarding the effects of extraction methods from the FEM models. The necessary assumptions are therefore elaborated in this paper. A number of issues regarding the stress extraction are addressed: Numerical errors, irregular meshes, choice of stress points, and the pile point of rotation.

The points for the *p-y* curves are computed by deforming the pile-soil system in two different ways. One method is to load the pile in a manner similar to that in the ULS situation of a real turbine. Hereby the pile is subjected to both a horizontal force and an overturning moment, both attacking at the pile top. This creates the most realistic deformation mode. However, only inappreciable deformations are created near the rotation point, causing difficulties extracting *p-y* curves at this location. The other method is applying a forced horizontal displacement of the entire pile as a solid body. Hereby significant deformations are ensured over the entire length of the pile. The failure mode when applying this method is not similar to the real situation though.

Two different material models are applied. The simple elastic perfectly plastic Mohr-Coulomb model is implemented, as this is the most common and fastest material model to use. The more sophisticated Hardening Soil model is also applied, as this may lead to more precise predictions of the soil behaviour.

The data from the FEM model is extracted from two different locations, in order to examine whether this has any influence on the extracted *p-y* curves. In the FEM model an infinitely thin interface is applied, from which the data can be extracted. This ensures collection of data at the actual pile-soil interface. In order to verify the curves extracted from the interface, data is also being collected from the soil elements. Data points at very close proximity of the pile are used, as this corresponds to the area of interaction, which the *p-y* curves seek to model.

Hereby the computed *p-y* curves are evaluated regarding the different extraction methods. The curves are furthermore compared to the conventional *p-y* curve methods described in the API.

CASE STUDY OF BARROW WIND FARM MONOPILE

The study is carried out as a case study of a monopile foundation for a wind turbine located at Barrow Offshore Wind Farm. The pile properties are estimated according to the foundation design report for the chosen wind turbine. The pile is a hollow steel cylinder with an embedded length of 29.4 m and an outer diameter of 4.75 m with a wall thickness of 0.1 m. This corresponds to a slenderness ratio, *L/D*, of approximately 6. A single load case from the extreme load analysis in the design report is chosen corresponding to maximum overturning moment at seabed. A horizontal force of 4656 kN and an overturning moment of 105656 kNm is applied. Torsional moment and bending moment around the *x*-axis are not considered in this paper.

The points for the *p-y* curves are computed by deforming the pile-soil system in two different ways. One method is to load the pile in a manner similar to that in the ULS situation of a real turbine. Hereby the pile is subjected to both a horizontal force and an overturning moment, both attacking at the pile top. This creates the most realistic deformation mode. However, only inappreciable deformations are created near the rotation point, causing difficulties extracting *p-y* curves at this location. The other method is applying a forced horizontal displacement of the entire pile as a solid body. Hereby significant deformations are ensured over the entire length of the pile. The failure mode when applying this method is not similar to the real situation though.

Two different material models are applied. The simple elastic perfectly plastic Mohr-Coulomb model is implemented, as this is the most common and fastest material model to use. The more sophisticated Hardening Soil model is also applied, as this may lead to more precise predictions of the soil behaviour. The data from the FE model is extracted from two different locations, in order to examine weather this has any influence on the extracted *p-y* curves. In the FE model an infinitely thin interface is applied, from which the data can be extracted. This ensures collection of data at the actual pile-soil interface. In order to verify the curves extracted from the interface, data is also being collected from the soil elements. Data points at very close proximity of the pile are used, as this corresponds to the area of interaction, which the *p-y* curves seek to model. Hereby the computed *p-y* curves are evaluated regarding the different extraction methods. The curves are furthermore compared to the conventional *p-y* curve methods described in the API.

Site Conditions

The soil parameters are estimated on basis of the boring profile and cone penetration test (CPT) conducted at the location of the pile. The pile is chosen on the argument that only cohesionless material is present in the soil layers. Both the Mohr-Coulomb parameters and the Hardening Soil parameters can be estimated entirely on basis of the CPT. The results from the CPT test show significant irregularities. The measurements have been stopped several times during the testing. This may be for numerous reasons. The tip resistance, q_c, may be too high due to occurrence of rocks or very dense layers. Furthermore the testing may have been stopped, so a soil test can be extracted. After each break in measurements, the cone must penetrate slightly into the soil, before the actual resistance of the soil is measured. Therefore the initial measurements after each break must be discarded, as they do not represent the correct response of the soil. Occasionally the q_c measurements experience peaks that do not represent the soil, without the testing being stopped. This may be due to occurrence of stones etc. These peaks must also be discarded. The accepted and discarded data points of the tip resistance of the CPT can be seen in Fig. 1.

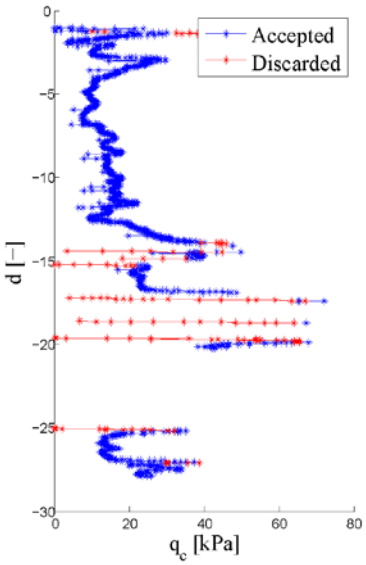

Fig. 1 Accepted and discarded data points for the q_c measurements.

The soil and strength parameters are determined using the proposed methods of Jamiolkowski et al. (2004) and Bolton (1986), in Eq.1, 2, and 3. However, the coefficient the lateral earth pressure at rest, K_0, is unknown. Therefore, an iterative procedure over Eq.1 through Eq.4 is executed. By implementing Eq. 4 it is assumed that the soil is normally consolidated. Eq.2 has been adjusted by Ibsen (2012)

$$D_r = \frac{1}{2.96}\ln\left(\frac{\frac{q_c}{P_a}}{24.94\left(\frac{\sigma'_{v0}\frac{1+2K_0}{3}}{P_a}\right)^{0.46}}\right) \quad (1)$$

$$\varphi'_{tr} = \varphi'_{crit} + 3°I_R - 3°D_r - \Delta\varphi_1 \quad (2)$$

$$I_R = D_r\left(Q_{min} - \ln\frac{p'}{1kPa}\right) - 1 \quad (3)$$

$$K_0 = 1 - \sin\varphi'_{tr} \quad (4)$$

where D_r is the relative soil density, σ'_{v0} is the initial vertical stress, and P_a is the atmospheric pressure. φ'_{tr} is the peak triaxial friction angle, φ'_{crit} is the critical angle of internal friction, I_R is the relative dilatancy index, $\Delta\varphi_1$ is a strength reduction due to silt content ,Q_{min} is a parameter adjusting for mineral strength and p' is the effective overburden pressure.

The value of φ'_{crit} is determined as recommended by Bolton (1986). The value of $\Delta\varphi_1$ corresponds to a silt content of 5-10 percent. Q_{min} is set to the value for quartz. A cap of 4 on the I_R values has been applied as recommended by Bolton (1986). The parameters, which need to be determined before the iteration, are listed in Table 1

Table 1 Predetermined parameters for the sand.

φ'_{crit} [°]	$\Delta\varphi_1$ [°]	Q_{min} [-]
33	2	10

A cap of 4 on the I_R values has been applied as recommended by Bolton (1986). The relative densities evaluated and the mean values for each layer are shown in Fig. 2. It is assumed that the mean values evaluated over the occasionally limited data within a layer represent the behaviour of the entire layer. All the remaining properties are inherently behaving in the same manner. The evaluated soil and strength parameters are listed in Table 2.

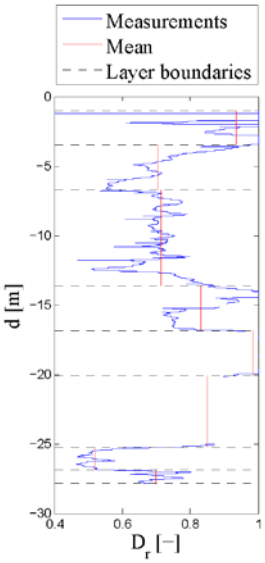

Fig. 2 Evaluated D_r and corresponding mean values at each layer.

Table 2 Strength and unit weight parameters evaluated on basis of CPT test. Effective cohesion, *c'*, is zero for all layers.

Soil Layer	K_0 [-]	γ [kN/m^3]	φ'_{tr} [°]	ψ [°]
1	0.32	19	42	12
2	0.34	19	41	12
3	0.31	19	43	12
4	0.31	21	43	12
5	0.32	21	42	12
6	0.32	21	42	12
7	0.32	19	42	11
8	0.31	19	43	12

The constrained modulus used in the Hardening Soil material model is calculated using Kulhawy and Mayne (1990) cf. Eq. 5. The remaining two moduli are calculated using Eqs. 5 and 6. Poisson's ratio, ν, in Eq. 6 is set to 0.3.

$$E_{oed} = q_c 10^{1.09 - 0.0075 D_r} \quad (5)$$

$$E_{50} = \frac{(1-2\nu)(1+\nu)}{1-\nu} E_{oed} \quad (6)$$

$$E_{ur} = 3E_{50} \quad (7)$$

The test data in Kulhawy and Mayne (1990) scatters compared to the fit in Eq.5, cf.Fig. 3. Therefore the evaluated stiffnesses may lead to a response in the FE model that differs from reality. The moduli will normally vary over the depth, following the shape of a power function, as given in Brinkgreve et al. (2012), Eqs. 8, 9, and 10.

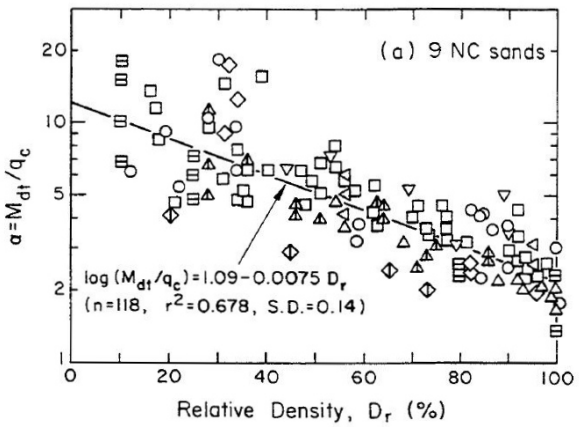

Fig. 3 Fit of E_{oed} function to data in mini-CPT tests. (Kulhawy and Mayne ,1990)

$$E_{oed} = E_{oed}^{ref}\left(\frac{c\cos\varphi - \frac{\sigma'_3}{K_0^{nc}}\sin\varphi}{c\cos\varphi + p^{ref}\sin\varphi}\right)^m \tag{8}$$

$$E_{50} = E_{50}^{ref}\left(\frac{c\cos\varphi - \sigma'_3\sin\varphi}{c\cos\varphi + p^{ref}\sin\varphi}\right)^m \tag{9}$$

$$E_{ur} = E_{ur}^{ref}\left(\frac{c\cos\varphi - \sigma'_3\sin\varphi}{c\cos\varphi + p^{ref}\sin\varphi}\right)^m \tag{10}$$

In Eq.8 p^{ref} is the primary principal stress, σ_1. In Eqs. 9 and 10 p^{ref} is the confining pressure. It is assumed that the confining pressure can be set to $K_0\sigma_{v0}$ and that $\sigma_1 = \sigma_{v0}$. According to Soos (1990) the power m can lie in the range $0.5 < m < 1.0$. This range of m will provide convex curves, giving moduli at gradually stabilizing values. At a given reference pressure, the reference moduli and m can be fitted to the values given by Eqs. 5 to 7. Such a fit is shown on Fig. 4. The reference pressure is set to σ_{v0} at the middle of the layer. The power law fits the data well with a power, m, of 0.5. The values regarding the moduli evaluated from the fit of the models of Eqs. 8 to 10 are given in Table 3. For the Mohr-Coulomb model, the modulus E' is set to the average value of E_{50} at each layer.

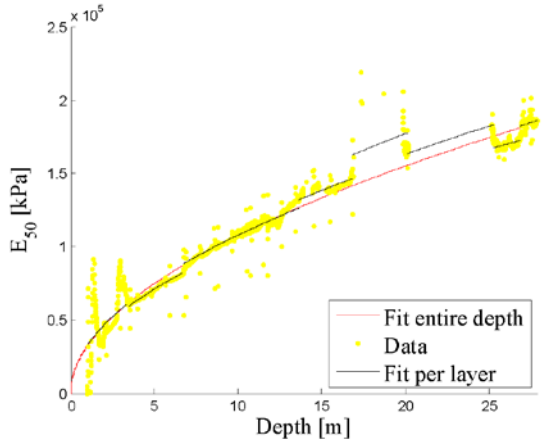

Fig. 4 Fitted model and computed values of E_{50}.

Table 3 Constitutive parameters for Hardening Soil and Mohr-Coulomb model evaluated on basis of CPT.

No.	E' [MPa]	E_{50}^{ref} [MPa]	E_{oed}^{ref} [MPa]	E_{ur}^{ref} [MPa]	p^{ref} [kPa]
1	3.5	3.8	2.0	10.2	24.4
2	3.6	4.1	3.0	12.8	80
3	5.7	6.2	4.0	18.0	178
4	7.8	8.2	5.5	24.2	277
5	9.2	9.5	6.4	28.7	342
6	8.6	8.8	5.9	26.5	424
7	8.8	8.9	6.1	26.7	491
8	10.4	10.6	7.1	31.9	516

NUMERICAL MODELLING OF MONOPILE

The Barrow Wind monopile is modelled by means of the commercial finite element program PLAXIS 3D. Model parameters are constructed according to the geometry and properties given for the pile. The monopile is modelled as a hollow steel cylinder constructed as structural plate elements with linear stiffness. Plate elements are two-dimensional 6-node triangular elements used to model thin two-dimensional structures. The plates are assigned a thickness in order to model the stiffness of the pile. The soil elements are 3D 10-node tetrahedral elements which correspond to 6 nodes at each of the sides of the tetrahedron. Interface elements are applied to the plate elements in order to model the soil-structure interaction properly. The interface elements consist of 12 nodes, a pair of 6-node triangular compatible with the 6-noded soil and structural elements. The strength and stiffness of the interface elements can be modified by a reduction factor, R_{inter}, in order to model the transition layer which is usually weaker than the surrounding soil. At the pile toe the interface elements are applied in extension of the plate elements. This is done to provide a flexible response and avoid stress concentrations (Brinkgreve et al., 2012). The boundary conditions are modelled so that no boundary effects are experienced when the analysis is run. By conducting preliminary tests it is ensured that the failure zone does not reach the boundaries of the numerical model. The soil layers found in the boring profile are extended horizontally across the model. The soil is divided into clusters to achieve a finer mesh near the pile. The sides of the model are restrained horizontally in their out-of-plane direction. The bottom surface is restrained in all directions. Bending moment loads cannot be applied directly in PLAXIS 3D. To comply with this limitation the pile head is extended above the soil surface so that the applied lateral load yields a moment force at the seabed according to the specified load case. The pile is loaded in the x-direction. A plate is added at the pile head in order to distribute the added load evenly onto the pile head. The load is applied at the centre of the top plate. The pile above seabed should have no structural influence on the embedded pile. To avoid second order effects from the pile above seabed it is assigned a high stiffness and very small unit weight. The resulting numerical model can be seen on Fig. 5.

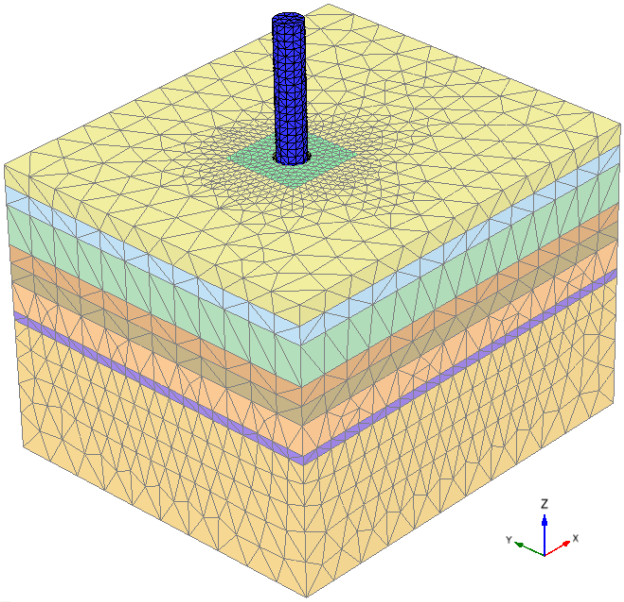

Fig. 5 The three-dimensional meshed model in PLAXIS 3D.

Method of Response Extraction from PLAXIS 3D

The calculation in PLAXIS 3D is controlled by means of phases. In order to obtain results that show the load-response development a number of successive phases, each with increasing load amplitude, are defined with the final phase being the extreme load case. For each phase stresses are extracted. The soil resistance, p, is taken as the x-component of the total stress acting at the circumference of the pile during loading. Each loading phase is followed by a plastic phase in which the load is removed and the average nodal plastic displacement in the pile structural elements at the given depth is taken as the pile deformation response, y. These phases define the plastic response of the soil by which the deformation is extracted.

Integration Method

Very few control parameters are available when meshing in PLAXIS 3D. The fineness can be controlled by introducing volumes with increased fineness, but the overall output is not controllable by the user. This means that the mesh output is rather random of nature and no symmetry can be introduced when evaluating stresses. When integrating stresses across the pile circumference one stress point may represent a larger element than the next. This would require extensive analyses of each nodal point for every evaluation of pile-soil response. A simple approach is to divide the pile into a number of slices for each depth of p-y curve evaluation. The height of the slice corresponds to the distance between each p-y curve. A slice of a stress evaluation can be seen in Fig. 6.

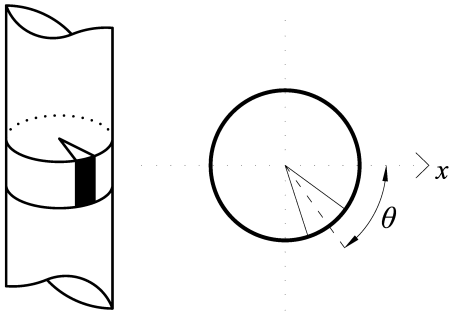

Fig. 6 A pile slice at a given depth of stress evaluation and the angle, θ, by which traction is evaluated for a pile slice related to load direction.

The slices are evenly distributed along the entire circumference and the arc length of each slice is relative to the number of slices introduced. Within each slice the traction is taken as the average traction of all present nodes. The angle, θ, by which the average traction is evaluated is the angular orientation of the slice in relation to the pile centre and the load direction, cf. Fig. 6. The number of slices is chosen by considering the number of stress points for the given mesh. For the mesh fineness applied in this analysis the interface consists of a total of 3600 stress points from which stresses are extracted. A certain number of stress points within each slice must be available for the average to be considered representative. In this way the effects of stress concentrations, as depicted in Fig. 7, can be reduced. This leads to restrictions regarding the maximum number of slices and p-y curves in proportion to the fineness of the mesh. The number of p-y curves is set to 20 which provide an average of 180 stress points per curve. A division into 16 slices is chosen which then provides an average number of stress points per slice of 11.25. This is considered as a reasonable representation of the average stress within each slice.

Extraction from Interface

Stresses in interface elements consist of effective normal stress, σ'_N, and shear stresses, τ_1 and τ_2. σ'_N is the effective normal stress acting normal to the interface surface. τ_1 is the shear stress acting along the circumference of the pile. τ_2 is the shear stress acting vertically along the length of the pile and are therefore not considered. PLAXIS 3D has difficulties simulating the cylindrical pile with the triangular elements. The corners of the structure elements peak out because they cannot enclose a perfectly circular shape. When the numerical analysis is run the effect of this can be seen as zones or stripes of stress concentrations scattered across the surface of the pile. The patterns are related to the stress points of the elements and are correlated with the element contours of the mesh. The stress concentrations increase when the mesh is coarsened as fewer elements around the pile circumference leads to increased angles between the surfaces. An example of the interface stress concentrations for a typical mesh fineness can be seen in Fig. 7.

It must be assured that these stress concentrations do not influence the result of the average pile-soil response without having to refine the mesh extensively. The lateral pile-soil response can be extracted from the model by evaluating stresses in either plates, interface or soil elements. Either method should give similar results given that the equilibrium between pile and soil must be fulfilled.

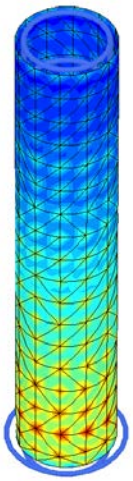

Fig. 7 Pile interface normal stress concentrations.

Extraction from Plates

Stresses in plate elements in PLAXIS 3D cannot be extracted directly as the structural response is evaluated as forces at the plate element integration points that are extrapolated to the element nodes (Brinkgreve et al., 2012). Stress evaluation of the plate elements would require establishment of the differential equations of shell elements by means of a finite difference method and is therefore not considered in this paper

Extraction from Soil

Stresses in soil elements are evaluated by considering the effective Cartesian stresses acting in the direction of the considered displacement, *x*. The considered stresses are the normal stress acting in *x*-direction, σ'_{xx}, and the shear stress acting on the *y*-plane in *x*-direction, σ'_{yx}. The shear stress acting on the *z* plane in *x*-direction, σ'_{zx} acts on the vertical plane *z* and is therefore not considered. The *x*-component stress at a point in the soil can be represented by the traction vector, T_x, at the pile surface expressed in Eq. 11. (Fan and Long, 2005)

$$T_x = \sigma'_{xx}\, n_x + \sigma'_{xy}\, n_y + \sigma'_{xz}\, n_z \tag{11}$$

σ'_{xx}, σ'_{xy}, and σ'_{xz} are Cartesian stresses (note that $\sigma'_{xy} = \sigma'_{yx}$ and $\sigma'_{xz} = \sigma'_{zx}$) and n_x, n_y, and n_z are components of unit normal along the *x*-, *y*-, and *z*-directions. These are given in Eq. 12 to 14 respectively.

$$n_x = \cos\theta_x \tag{12}$$

$$n_y = \cos\theta_y \tag{13}$$

$$n_z = \cos\theta_z \tag{14}$$

θ is the angular orientation of the stress point in relation to the pile centre. The total soil response, p_x, per unit length of pile, which corresponds to the subgrade reaction, is found by integrating the soil resistance over the pile circumference at given depth during loading. When extracting stresses from the surrounding soil elements, the stresses cannot be evaluated at the exact circumference of the pile. In order to obtain an adequate amount of stress points within each integration area, cf. Fig. 6, stress points at a certain distance from the pile must be implemented. This issue is illustrated in Fig. 8. Being that the stress points are further from the pile, forces are distributed to a larger area. This means that stresses become lower. The response obtained from the soil elements are therefore expected to be slightly lower than those obtained from the interface.

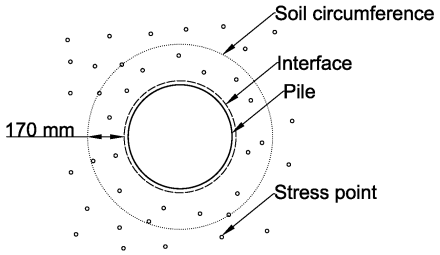

Fig. 8 Required circumference for obtaining sufficient stress points in soil.

Comparison of Extraction Methods

Fig. 9 and Fig. 10 shows the calculated soil resistances from interface elements for a depth of 3.9 m at load step 500 kN in the MC model analysis. The out-of-plane normal stress, σ'_N, in Fig. 9a shows a small stress at the back side of the pile and the largest stresses at the front side corresponding the active and passive pressure respectively. The *x*-component of the out-of-plane stress, $\sigma'_{N,x}$, in Fig. 9b, shows that the contributions from the sides of the pile reduce to near zero values. Similarly in Fig. 10a, the radial shear stress, τ_r, is largest on the side of the pile and are near zero on the front and back of the pile. As a result the *x*-component of the radial shear stress, $\tau_{r,x}$, in Fig. 10b is close to τ_r. The soil resistances for all slices are integrated over the pile circumference yielding the subgrade reaction for the given depth.

An example of the subgrade reactions evaluated by means of interface and soil elements respectively can be seen in Fig. 11. There is some difference between the two curves of the subgrade reactions originating from the fact that the stresses in the soil elements are evaluated at a distance from the pile. At the bottom of the pile some deviation is observed which is related to the complex behaviour of the soil in this area.

On basis of Fig. 11 the soil resistance evaluated from interface elements are preferred over soil resistance evaluated from soil elements. The corresponding pile deflection at load step 500 kN and a fitted linear line are seen in Fig. 12. It is seen that the pile behaves almost rigid as depicted with a point of rotation and a slight curve compared to the fitted line.

Pile Excitation by Forced Displacement

Non-slender piles during lateral loading exhibit rigidly behaviour and rotate around a point of zero deflection forming a soil wedge as depicted in the possible failure mode in Fig. 13. An issue when constructing *p*-*y* curves by means of finite element modelling is the evaluation of soil response in proximity to the pile rotation point.

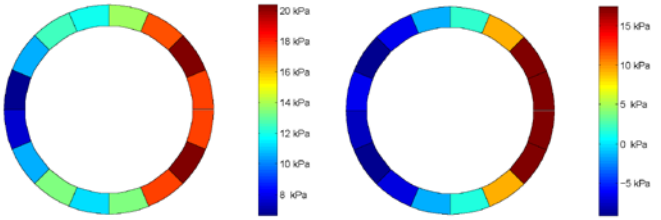

Fig. 9 a) Out-of-plane normal stress, σ'_N b) x-component, $\sigma'_{N,x}$ Interface response for MC model at depth 3.9 m, load step 500 kN. Right-hand side is active side of pile.

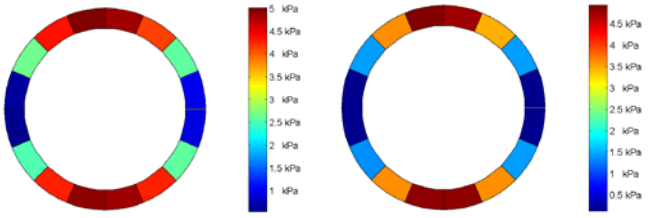

Fig. 10 a) Radial shear streess, τ_r b) x-component, $\tau_{r,x}$ Interface response for MC model at depth 3.9 m, load step 500 kN. Right-hand side is active side of pile.

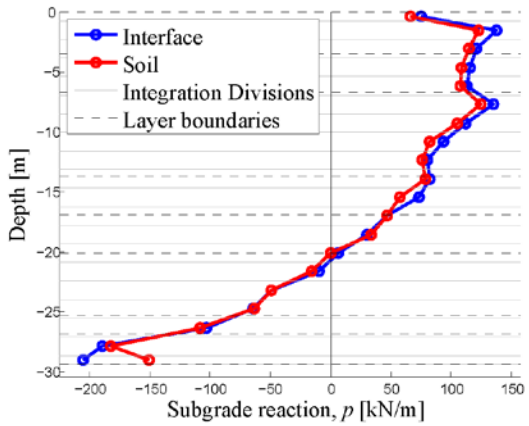

Fig. 11 Subgrade reactions along depth of pile evaluated from interface and soil elements, respectively, load step 500 kN.

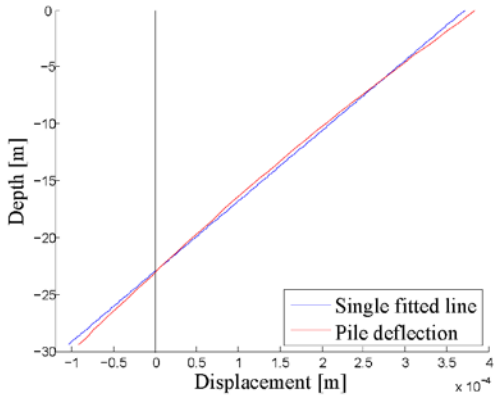

Fig. 12 Pile deflection at load step 500 kN

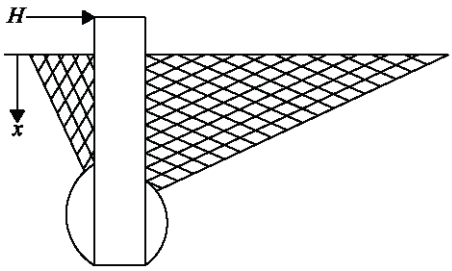

Fig. 13 Possible failure mode for a smooth surfaced, non-slender pile at shallow depth (Sørensen et al., 2012).

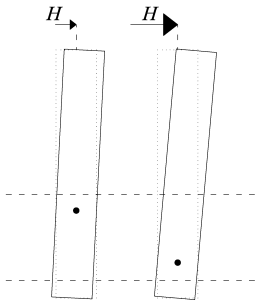

Fig. 14 Schematic of the range of possible rotation points for different load amplitudes.

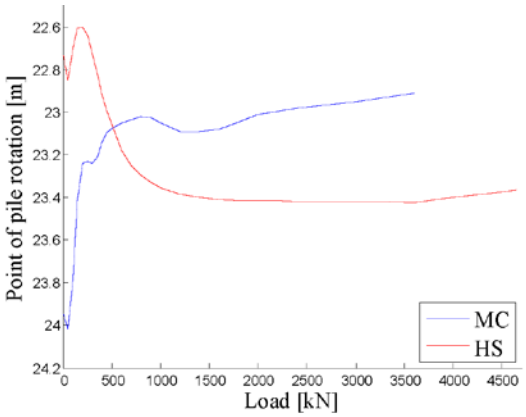

Fig. 15 Point of pile rotation for the MC model and HS model respectively.

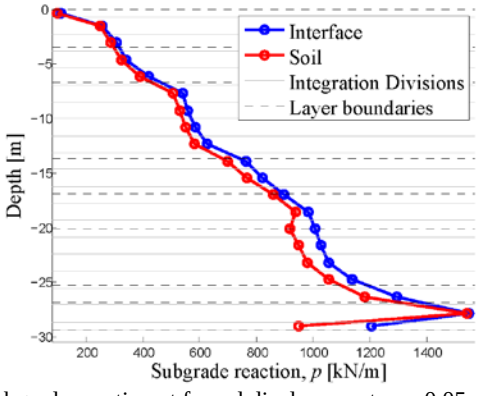

Fig. 16 Subgrade reaction at forced displacement, y = 0.05 m.

In the finite element model this results in the soil response being irregular near the point of rotation. The location of this point changes when applying different load amplitudes as exemplified in Fig. 14. The location of this point changes when applying different load amplitudes. The varying location of the point of pile rotation for the load case for both the MC model and the HS model is shown in Fig. 15. Around the point of pile rotation the subgrade reactions are close to zero, cf. Fig. 11. At depth near the point of rotation, displacements and subgrade reactions representing the entirety of a *p-y* curve cannot be achieved. Due to this, the *p-y* curves are difficult to extract when applying a horizontal load. In order to cope with this issue an appropriate forced displacement may be applied to the pile in order to simulate the necessary pile excitation.

A forced displacement is applied to the entire pile surface in the direction of load. The measured response is taken as the *p-y* behaviour, where *p* is the resulting subgrade reaction during the forced displacement and *y* is found as the plastic displacement after the forced displacement is removed. The resulting subgrade reactions along the pile length for a given forced displacement can be seen in Fig. 16. It is observed from that the subgrade reaction increases with depth and that it does not reach zero at any point. Similar to the observation during loading in Fig. 11 deviations are visible near the pile bottom. In Fig. 17 the extracted *p-y* curves from the forced displacement are depicted together with curves extracted from the load case for three different depths, i.e. 1.5 m, 7.7 m, and 29 m, respectively. The *p-y* curve at a depth of 1.5 m shown in Fig. 17a displays a much stiffer response for the load case. At depth 7.7 m, Fig. 17b, the responses are almost identical. At depth 29 m in Fig. 17c a negative response is observed for the load case which is related to the toe kick. For the load case it is also noticed that the amount of deflection, *y*, is much less than that depicted for a depth of 1.5 m in Fig. 17a. Not shown here, the *p-y* curves close to the pile rotation point for the load case show even smaller deflection and an unreliable response. It is not possible to make reliable conclusions regarding the response for the load case in this area. Thus, the choice of excitation method for *p-y* curve evaluation should be the forced displacement when near the point of pile rotation. Near the top and bottom of the pile the load case is applicable and should be the choice as it represents the actual failure mechanism.

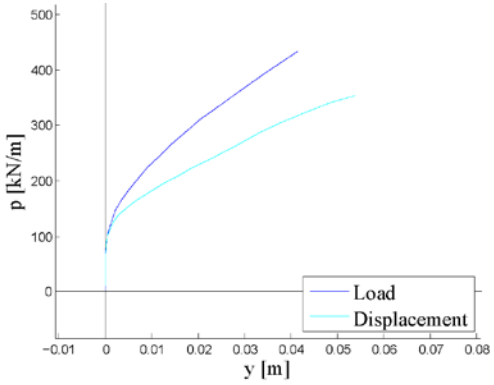

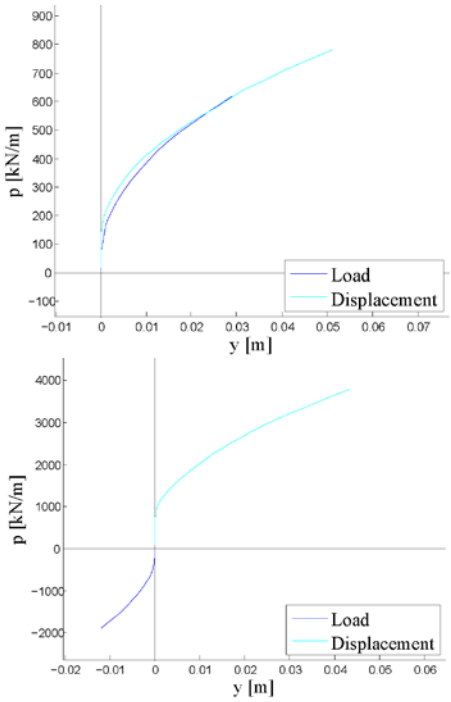

Fig. 17 *p-y* curves determined by means of the MC model for load and forced displacement respectively.

Comparison of Material Models

Another observation in Fig. 17 is the near vertical initial response of the *p-y* curves. This is observed at all depths for the *p-y* curves computed for the MC analysis. The observation is related to the elastic perfectly plastic behaviour of the MC model. At excitations up to a certain threshold the pile exhibits almost zero plastic deformation. Based on this observation the *p-y* behaviour of the MC model is considered unreliable. Analysis results with inclusion of a HS model in the analysis results at a depth of 7.7 m is shown on Fig. 18. The pile exhibits immediate plastic response which corresponds to the hyperbolic stress-strain relation in the stiffness behaviour of the HS model. This results in a response less stiff than obtained by the MC model.

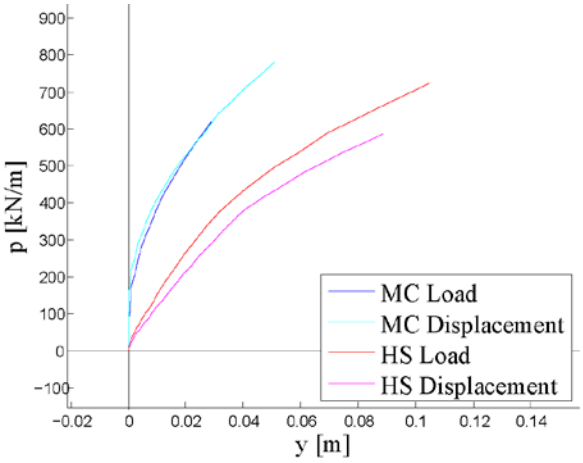

Fig. 18 *p-y* curves determined by means of the MC model and HS model respectively.

Comparison of Soil Response with API Method

The *p-y* curves obtained from the finite element model are set against the curves obtained by the traditional method of API (2010). This juxtaposition for a shallow depth can be seen on Fig. 19.

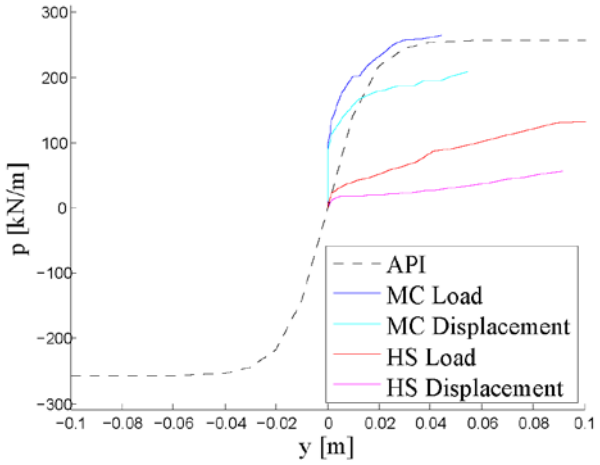

Fig. 19 *p-y* curves at d = 0.4 m.

Here the Mohr-Coulomb curves seem to fit well with the API curve. However, the issue regarding the infinite initial modulus of the MC-curve is present. The HS curves show a respond that is significantly less stiff than the API curves. This suggests that API (2010) overestimates the initial subgrade modulus, E^*_{py}, at shallow depth. At greater depths this difference becomes more substantial. At approximately half the pile depth, the methods disagree considerably. This is seen on Fig. 20.

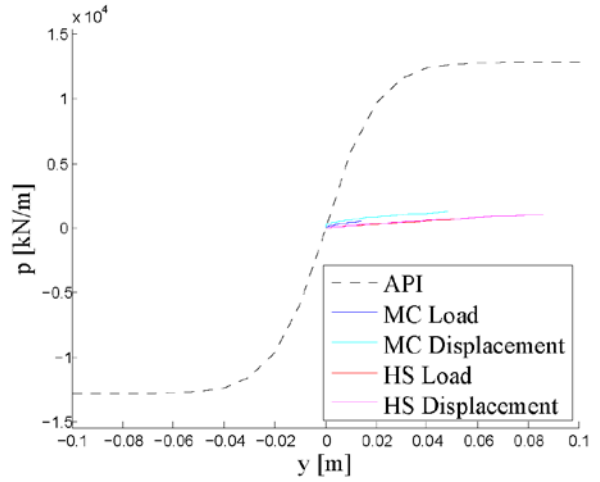

Fig. 20 *p-y* curves at d = 15.5 m.

This pattern indicates that the assumed linear increase of initial subgrade modulus in API (2010) greatly overestimates the stiffness of the response. However, caution should be taken, when comparing the obtained results with API (2010). The finite element model has not been validated. As no test results for the simulated pile are available, the output of the model cannot be deemed verified. The extraction method needs validation as well. The obtained *p-y* curves must be incorporated in a Winkler model, and the response must be held up against the response given directly from the FEM model. The exact values from the model cannot be deemed fully reliable. Nevertheless, the general shapes of the curves, and the behaviour over the depth of the pile are believed to be representative of the true behaviour.

CONCLUSION

In this paper a numerical analysis of a laterally loaded monopile in sand is conducted. The analysis is conducted by means of the finite element program PLAXIS 3D. A case study of a full-scale wind turbine is provided as the subject for research. A method for extracting *p-y* curves by evaluating stress points is presented. Two different excitations, applied load and forced displacement, are utilised in order to evaluate *p-y* curves. *p-y* curves are evaluated by means of two material models in the numerical analysis: The Mohr-Coulomb model and the Hardening Soil model. Finally, the extracted *p-y* curves are compared to the *p-y* curves formulated in the API. The general conclusions are:

Stress concentrations in the interface elements in PLAXIS 3D are observed. They are related to the modelling of curved structures in the finite element formulation. The method for extracting *p-y* curves considers the average stresses in order to cope with this. The slices conducted in the method for extracting *p-y* curves produce stress results that fit reasonably with the expected traction on the pile surface. The *p-y* curves evaluated from forced displacement provide the best basis for extraction of *p-y* curves along the entire length of the pile

Near the top and bottom of the pile, using applied load as excitation method must be recommended, due to the misleading failure mode of a forced displacement in these areas. The deflection of the pile consists of rigid body motion during loading. A slight curvature is noticed.

The Mohr-Coulomb model shows no plastic deformation in a considerable range of loading due to its bilinear stress-strain curve. The Hardening Soil model provides immediate response which results in less stiff *p-y* curves.

The conventional *p-y* curves formulated in API shows a much stiffer response at depth than either of the applied material models and excitation methods. This may be related to the linearly increasing initial subgrade modulus, E^*_{py}.

AKNOWLEDGEMENT

This research is associated with the EUDP programme “Monopile cost reduction and demonstration by joint applied research” funded by the Danish energy sector. The financial support is sincerely acknowledged.

REFERENCES

API (2010). “Recommended Practice for Planning, Designing and Constructing Fixed Offshore Platforms-Working Stress Design, RP 2A-WSD”, 21st edn, American Petrolium Institute.

Bolton, M. D., 1986 “The strength and dilatancy of sands” *Geotechnique 36 no. 1*, pp. 65-78, 1986

Brinkgreve, R. B. J., Engin, E., and Swolfs, W. M., 2012 “Plaxis 3D 2011 Manual”

DNV (2010). “Offshore standard DNV-OS-J101: Design of offshore wind turbine structures”. *Technical report DNV-OS-J101”*, Det Norske Veritas.

Fan C. C. and Long J. H., 2005 “Assessment of existing methods for predicting soil response of laterally loaded piles in sand”, *Computers and Geotechnics 32*, pp. 274-289.

Hald, T., Mørch, C., Jensen, L., Bakmar, C. L. and Ahle, K., 2009 “Revisiting monopile design using p-y curves – Results from full scale measurements on Horns Rev“ *European Offshore Wind Conference & Exhibition 2009*, Stockholm, Sweden, Vol. 3 pp. 1926-1935.

Ibsen, L. B. 2012 –Notes from PhD Course “Behaviour and Properties of Natural Soils” January 2012, Department of Civil Engineering, Aalborg University, Denmark.

Jamiolkowski, M, Lo Presti, D. C. F and Manassero, M., 2004 “Evaluation of Relative Density and Shear Strength of Sands from CPT and DMTI” Soil Behaviour and Soft Ground Construction: Proceedings of the Symposium, No. 119, American Society of Civil Enginners, pp.201-238

Kulhaway, F. H. and Mayne, P. W., 1990 “Manual Estimating Soil Properties for Foundation Design” Report EL6800, Electric Power Research Institute, Palo Alto, USA.

McGann, C., Arduino, P. and Mackenzie-Helnwein P., 2011, “Applicability of Conventional p-y Relations to the Analysis of Piles in Laterally Spreading Soil” *Journal of Geotechnical and Geoenvironmental Engineering* 137(6), pp. 557-567.

Moreno, A. B., Mikalauskas, L., and Diaz J. L. T, 2011, “Experimental and Numerical Evaluation of the behavior of laterally-loaded non-slender piles” *MSc Thesis*, Department of Civil Engineering, Aalborg University, Denmark.

Sørensen, S. P. H., Møller, M., Brødbæk, K., Augustesen, A. H. and Ibsen, L. B. 2009, “Evaluation of Load-Displacement Relationships for Non-Slender Monopiles in Sand”. *DCE Technical Report No. 79*, Aalborg University. Department of Civil Engineering.

Sørensen, Brødbæk, Møller, Augustesen, 2012, “Review of laterally loaded monopiles employed as the foundation for offshore wind turbines”.

von Soos, P. 1990, Properties of Soil and Rock (in German), Grundbau Taschenbuch Part 4. Edition 4, , Ernst & Sohn, Berlin

Recent publications in the DCE Technical Memorandum Series

ISSN 1901-7278
DCE Technical Memorandum No. 024